LXR agonist suppresses atherosclerotic lesion growth and promotes lesion regression in apoE*3Leiden mice: time course and mechanisms[S]

Lars Verschuren,[*,†] Jitske de Vries-van der Weij,[*,§] Susanne Zadelaar,[*] Robert Kleemann,[*] and Teake Kooistra[1,*]

Netherlands Organisation for Applied Scientific Research (TNO) Quality of Life,* Biosciences, Leiden, The Netherlands; and Departments of Vascular Surgery,† and Human Genetics,§ Leiden University Medical Center, Leiden, The Netherlands

Abstract **The aim of this study was to define the anti-atherosclerotic role of liver-X-receptors (LXRs) under lesion progressive and lesion regressive conditions, to establish a temporal line of events, and to gain insights into the mechanisms underlying the anti-atherogenic potency of LXRs. We used apoE*3Leiden (E3L) mice to comprehensively and time-dependently dissect how T0901317, an LXR-agonist, inhibits initiation and progression of atherosclerotic lesions and regresses existing lipid- and macrophage-rich lesions. T0901317 suppresses lesion evolution and promotes lesion regression regarding lesion number, area, and severity. Quantitative plasma and vessel wall analyses corroborated by immunohistochemical evaluation of the aortic lesions revealed that under progressive (high-cholesterol diet) as well as regressive (cholesterol-free diet) conditions T0901317: *i*) significantly increases plasma triglyceride and total cholesterol levels; *ii*) does not affect the systemic inflammation marker, Serum amyloid A (SAA); *iii*) suppresses endothelial monocyte adhesion; and *iv*) induces the expression of the cholesterol efflux-related genes apolipoprotein E (apoE), ATP binding cassette (ABC) transporters ABCA1 and ABCG1. Furthermore, under progressive conditions, T0901317 suppresses the vascular inflammatory status (NF-κB) and the vascular expression of adhesion molecules [E-selectin, intercellular adhesion molecule (ICAM)-1, and CD44], lowers lesional macrophage accumulation, and blocks lesion evolution at the transition from lesional stage II to III. Under regressive conditions, T0901317 induces lesional macrophage disappearance and increases the expression of the chemokine receptor CCR7, a factor functionally required for regression. The LXR-agonist T0901317 retards vascular lesion development and promotes lesion regression at several levels. The findings support that vascular LXR is a potential anti-atherosclerotic target.**—Verschuren, L., J. de Vries-van der Weij, S. Zadelaar, R. Kleemann, and T. Kooistra. **LXR agonist suppresses atherosclerotic lesion growth and promotes lesion regression in apoE*3Leiden mice: time course and mechanisms.** ***J. Lipid Res.*** **2009.** 50: **301–311.**

Supplementary key words atherosclerosis • liver-X-receptor • inflammation • macrophages

Coronary atherosclerosis represents the leading cause of morbidity and mortality of men and women throughout the Western world. Hypercholesterolemia is a well-established risk factor for the incidence of atherosclerosis and its pathologic complications (1). However, despite the success of cholesterol-lowering statins in reducing cardiovascular causes of death, two-thirds of the statin-treated patients still experience cardiovascular events. Consequently, focus has switched to risk factors other than hypercholesterolemia.

Atherosclerosis is now recognized as a multifactorial, multistep disease with numerous etiologies that have to act in concert to initiate and promote the atherosclerotic process. In addition to traditional risk factors, such as hypertriglyceridemia, low HDL, and hypertension, inflammation is accepted as a major driving force of atherosclerotic lesion development. Inflammation has a key role in lesion initiation and evolution, and encompasses cellular and molecular components (2).

Liver-X-receptor (LXR) belongs to the nuclear hormone receptor superfamily of ligand-activated transcription factors. Two LXR isoforms have been described so far, LXRα and LXRβ. LXRβ has a ubiquitous tissue distribu-

The Dutch Heart Foundation (NHS; grant 2002B102 to L.V.), the Center for Medical Systems Biology CMSB (grant 115 to J.d.V.-v.d.W), the Dutch Organization for Scientific Research (NWO; grant VENI 016. 036.061 to R.K.), the European Nutrigenomics Organisation NuGO (CT-2004-505944; grants to S.Z, R.K., and T.K.) a Network of Excellence funded by the European Commission's Research Directorate General (Sixth Framework Programme for Research and Technological Development) and TNO Research Program NISB (to R.K. and T.K..

Manuscript received 16 July 2008 and in revised form 29 August 2008.

Published, JLR Papers in Press, August 30, 2008.
DOI 10.1194/jlr.M800374-JLR200

[1] To whom correspondence should be addressed.
e-mail: Teake.Kooistra@tno.nl

[S] The online version of this article (available at http://www.jlr.org) contains supplementary Materials and Methods and a supplementary table.

tion, whereas LXRα predominates in liver, adipose tissue, intestinal tissue, and macrophages; both isoforms respond to the same natural and synthetic ligands (3). LXRs control genes involved in intestinal cholesterol absorption, hepatic bile acid synthesis, cholesterol efflux, vascular foam cell formation, and inflammation (4). These properties make LXRs a potential target for therapeutic intervention in the atherosclerotic process. Studies performed over the last several years have established that LXRs are anti-atherosclerotic factors owing to their ability to regulate cholesterol and lipid homeostasis and to inhibit inflammation within the arterial wall (5–8). However, these studies focused on lesion growth, but not lesion regression, did not establish a temporal line of events and only partly addressed the mechanisms underlying the anti-atherogenic potency of LXRs.

Here we describe the impact of an LXR-agonist, T0901317, on the progression and regression of atherosclerosis in transgenic apoE*3Leiden (E3L) mice, a well-established mouse model for atherosclerosis (9, 10). E3L mice are highly responsive to cholesterol-containing diets, resulting in strongly elevated plasma cholesterol and triglyceride levels, with a prominent increase in VLDL- and LDL-sized lipoprotein particles. E3L mice do not develop atherosclerosis on a regular chow diet, but atherosclerosis in E3L mice can be initiated by feeding of a cholesterol-containing, Western-type diet (9), whereas regression of pre-existing lesions can be induced using cholesterol-depleted diets (11). E3L mice respond to hypolipidemic drugs with cholesterol lowering and appear useful in predicting effects of pharmaceutical modifiers in humans (9). Our study confirms the results previously published by other groups in different mouse models [apolipoprotein E (apoE)$^{-/-}$ or LDLr$^{-/-}$ mice] regarding some of the effects of LXR-agonists on lesion development, but adds some important information with regard to the action of the LXR-agonist on the vasculature, in particular to vascular inflammation, adhesion molecule expression, and under regressive conditions, potential mechanisms involved in macrophage disappearance. Also, the analysis of the experiments at different time points allowed establishing of a temporal line of events.

MATERIALS AND METHODS

See the online-only supplementary data for an expanded Methods section.

Animals

Female E3L transgenic mice (Netherlands Organisation for Applied Scientific Research) were characterized for expression of human apoE by enzyme-linked immunosorbent assay. Animal experiments were performed according to the *Guide for the Care and Use of Laboratory Animals* (NIH-Publication No.-85-23, revised 1996) and approved by the institutional Animal Experimental Committee.

T0901317-Atherosclerosis studies

Progression studies. To establish a time course of events, three separate progression studies were performed, with mice (age 10–12 weeks at start of experiment) sacrificed after t = 2 weeks, t = 10 weeks, or t = 15 weeks of experimental treatment, respectively.

Study 1 (main study; sacrifice at 10 weeks). During a run-in period of 3 weeks, 24 female E3L mice received an atherogenic, 1% (w/w) cholesterol-containing Western-type diet (Hope Farms, Woerden, The Netherlands), further referred to as high-cholesterol (HC) diet. Then, mice were subdivided into two experimental groups (n = 12) and matched for plasma cholesterol and triglycerides. In one group, HC was continued for another 10 weeks (HC group). The other, T0901317-treated group (HC+T0901317 group) received HC supplemented with 0.01% w/w T0901317 (Sigma Aldrich). Based on food intake in the HC+T0901317 group, the daily dose of T0901317 was 11 mg/kg bodyweight.

Study 2. As study 1, but sacrifice at 15 weeks; n = 15 per group.

Study 3 (short study; sacrifice at 2 weeks). E3L mice were treated with HC-diet supplemented with or without 0.01%(w/w) T0901317 (n = 8 per group; no run-in) and were sacrificed after 2 weeks of treatment.

Regression study. Twenty-six female E3L mice received HC for 18 weeks to develop atherosclerotic lesions. Then, 10 mice were sacrificed for atherosclerotic lesion analysis. The 16 remaining mice were subdivided into two groups of 8 mice each and switched for 8 weeks to a regressive, cholesterol-depleted diet (RD), supplemented with 0.01% (w/w) T0901317 (RD+T0901317 group) or not (RD group).

Statistical methods

Significance of difference was calculated by ANOVA test followed by a least significant difference post hoc analysis using SPSS 11.5 for Windows (SPSS, Chicago, IL). The level of statistical significance was set at $P < 0.05$.

RESULTS

T0901317 enhances plasma lipid levels in E3L mice

Food intake of mice fed HC+T0901317 for 10 weeks was slightly lower than that in animals on HC (2.2 ± 0.2 g per day (g/day) vs. 2.5 ± 0.2 g/day; $P < 0.05$; see supplementary Table I). At the end of the treatment period, there was no significant difference in body weight between the two groups (HC+T0901317, 19.6 ± 0.5 g; HC, 20.8 ± 0.4 g; see supplementary Table I). Plasma cholesterol levels in HC+T0901317 (23.4 ± 4.1 mM) were significantly increased compared with HC (18.7 ± 3.6 mM, $P < 0.05$; see supplementary Table I). This rise in plasma total cholesterol levels in HC+T0901317 can be mainly ascribed to a particular subfraction (fractions 10–17; **Fig. 1A**), coeluting with particles in the intermediate density lipoprotein (IDL)/LDL range. T0901317 strongly (6.8 times) increased fasting plasma triglyceride levels (HC+T0901317, 12.3 ± 4.4 mM; HC, 1.8 ± 0.4 mM; $P < 0.05$; see supplementary Table I), which rise is entirely confined to particles in the VLDL-range (Fig. 1B). Quantitative RT-PCR analysis of liver samples indicates that the strong increase in triglyceride levels in the T0901317-treated group may at least partly be explained by the 2.2-fold ($P < 0.01$) elevated expression of the lipogenic gene, sterol regulatory element binding protein (SREBP)-1c.

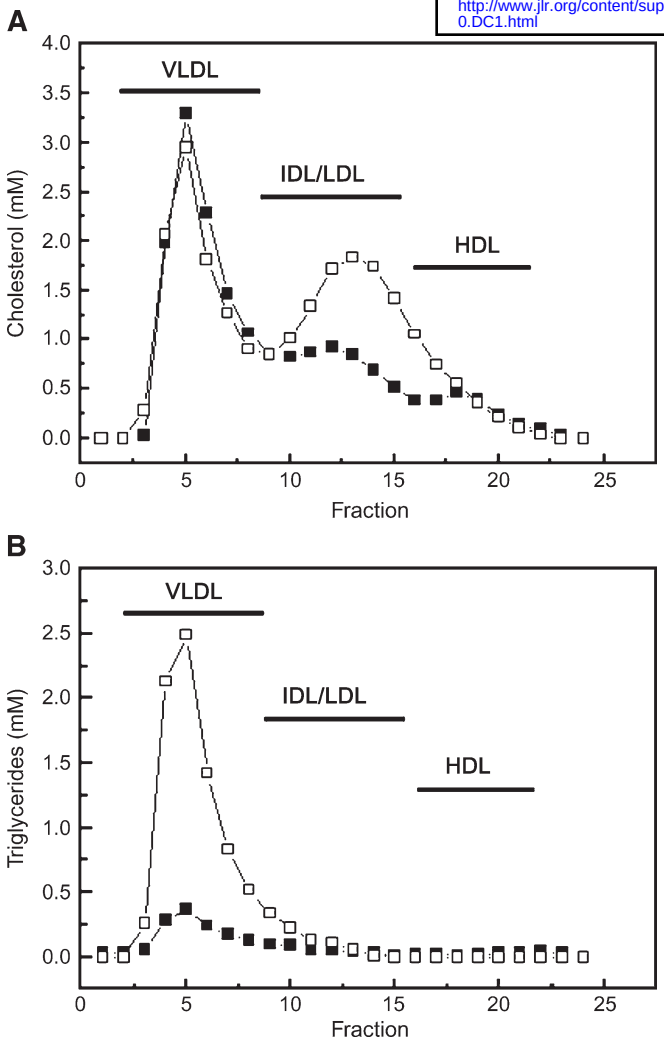

Fig. 1. Lipoprotein profiles of control and T0901317-treated, cholesterol-fed apoE*3Leiden (E3L) mice. Shown are the lipoprotein profiles measured after separation by fast-performance liquid gel-filtration chromatography of pooled plasma of the two experimental groups (n = 12 for each group) at the end of the 10-week treatment period. A: Cholesterol content in fractionated plasma samples. B: Triglyceride content in fractionated plasma samples. Solid squares indicate HC; open squares indicate HC+T0901317.

T0901317 reduces atherosclerotic lesion number, size, and severity

After 10 weeks of experimental treatment, early atherosclerotic lesion formation was analyzed in cross-sections of the aortic valve area. The average lesion number per mouse was 18.3 ± 2.3 in HC and reduced by 64% to 6.5 ± 1.3 in HC + T0901317 ($P < 0.01$; **Fig. 2A**). Measurement of the total cross-sectional lesion area showed a similar picture (Fig. 2B): HC displayed a cross-sectional lesion area of 37027 ± 7450 μm^2 and HC+T0901317 reduced the lesion area by 85% to 5484 ± 2019 μm^2 ($P < 0.05$).

To assess whether these differences reflect a difference in time of onset of the disease process or are the result of diminished lesion initiation and progression, lesion number and size were also analyzed (in a separate experiment) after a 15-week treatment. The difference in lesion number of the two groups resembled that of the 10-week experiment (Fig. 2C), while the lesion area was substantially increased in HC (3.2-fold) but only marginally (1.5-fold) in HC+T0901317 after 15 weeks (Fig. 2D), indicating that T0901317 is interfering with lesion initiation and lesion development rather than retarding the onset of the disease process.

This conclusion was further strengthened by evaluating lesion severity. Cross-sections of the aortic root were morphologically analyzed, and lesions were graded according to the classification of the American Heart Association (12). Grading after 10 weeks demonstrated that lesions from HC and HC+T0901317 mainly contained mild-type I/II lesions (~80% of all classified lesions) and hardly type IV/V lesions (Fig. 2E). After 15 weeks, a clear shift in lesion severity was observed in HC but not in HC+T0901317. In HC, 24% ± 6% of all cross-sections contained type I/II lesions and 76% ± 5% contained type III/IV/V lesions (Fig. 2E). In contrast, in HC+T0901317 treated mice 77% ± 10% of all cross-sections contained type I/II lesions and 23% ± 4% contained type III/IV/V lesions, thereby remarkably resembling the findings obtained after the 10-week treatment. Importantly, T0901317 blocked lesion progression at the transition from lesion severity stage II to III, which is characterized by the absence of smooth muscle cell (SMC) proliferation and migration to the cap, a hallmark of type III lesions.

Thus, T0901317 strongly suppresses atherogenesis, at the initiation and the progression phase of disease. The question therefore arises by what mechanism T0901317 interferes with the atherosclerotic process.

The vessel wall as target for T0901317

To evaluate whether the anti-atherosclerotic effects of T0901317 are paralleled by anti-inflammatory effects, we analyzed systemic inflammatory markers originating from liver (SAA) or vasculature (E-selectin). HC markedly and significantly elevated plasma levels of both SAA (2.1-fold) and E-selectin (1.2-fold) (**Table 1**). T0901317 significantly suppressed HC-induced E-selectin but not SAA plasma levels, pointing to a direct anti-inflammatory effect of T0901317 on the vascular endothelium.

To seek further evidence for a direct effect of T0901317 on the vessel wall, we evaluated vascular expression of LXRα/β immunohistochemically using an antibody recognizing both LXR isoforms (see Materials and Methods section). In chow-fed E3L mice, no LXRα/β expression was detectable in the vasculature (**Fig. 3A**), but 2 weeks after starting the HC diet, expression of LXRα/β was demonstrable in the HC and HC+ T0901317 group (Fig. 3B, C) and remained so for the rest of the experimental treatment period (Fig. 3D, E). In both experimental groups, expression of LXRα/β was mainly confined to the endothelium and to a lesser extent to SMC; no notable difference in staining intensity was seen between the two groups (Fig. 3B–E). Upon lesion progression, accumulating monocyte-derived macrophages in the lesions also stained positive for LXRα/β (Fig. 3F). Quantitative RT-

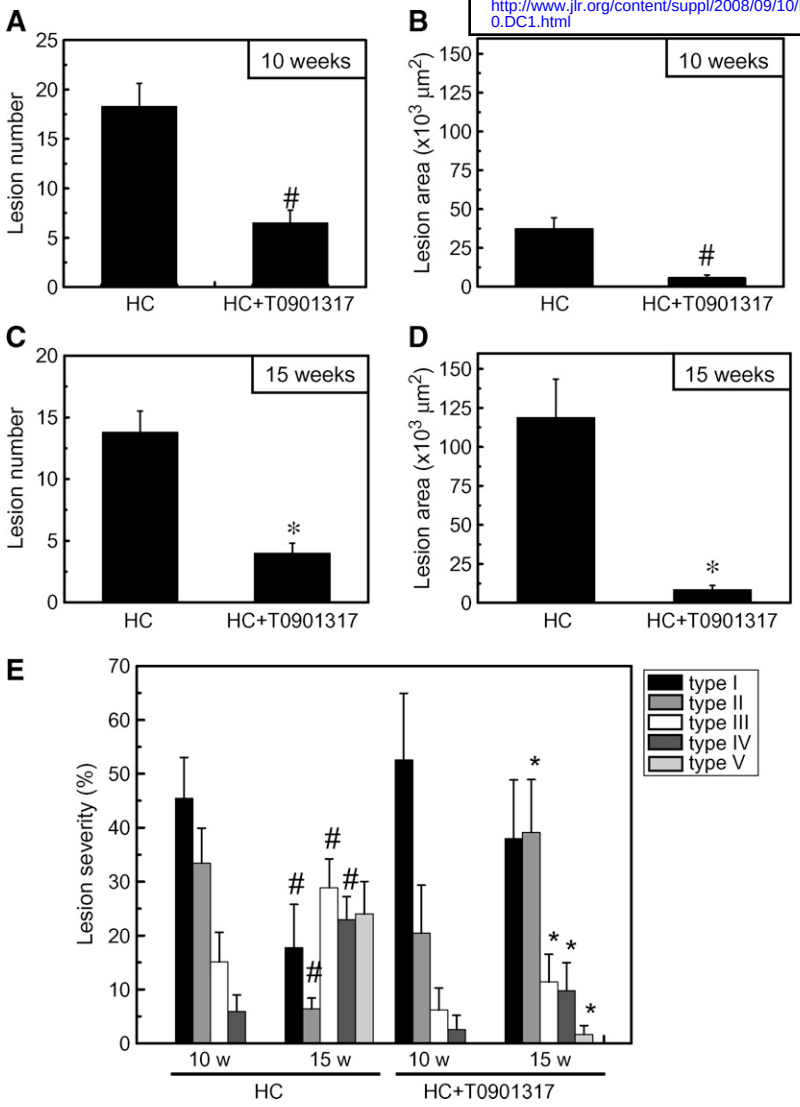

Fig. 2. Effect of T0901317 on atherosclerosis development in aortic valve area. Shown are effects of T0901317 on total lesion number after 10 weeks (A) and 15 weeks (C) of treatment and effects of T0901317 on total cross-sectional lesion area after 10 (B) and 15 weeks (D) of treatment. The effect of T0901317 on lesion severity is presented as percentage of cross-sections analyzed (E). Data represent mean values ± SEM (n = 10 mice per group). # $P < 0.05$ vs. HC-10 weeks, * $P < 0.05$ vs. HC-15 weeks.

PCR analysis revealed that both LXRα and LXRβ were approximately 2-fold up-regulated by dietary cholesterol.

Together, these data demonstrate that dietary cholesterol induces LXR protein expression in the vasculature (endothelium, SMC, monocyte-derived macrophages), thus enabling T0901317 to specifically suppress HC-induced expression of endothelial E-selectin and thereby to lower plasma levels of E-selectin.

TABLE 1. Effect of T0901317 on plasma inflammation markers

	t = 0	HC	HC+ T0901317
Serum amyloid A (µg/ml)	10.1 ± 4.6	21.7 ± 15.3[a]	24.5 ± 12.1[a]
E-selectin (ng/ml)	84.4 ± 9.7	97.2 ± 13.7[a]	84.4 ± 12.2[b]

Plasma inflammation markers of control and T0901317-treated, cholesterol-fed apoE*3Leiden (E3L) mice. Shown are average plasma levels of serum amyloid A and E-selectin at the start (t = 0) and the end (t = 10 weeks) of the treatment period (means ± SD; n = 12 for each group).

[a] $P < 0.05$ vs. t = 0.

[b] $P < 0.05$ vs. HC.

Anti-atherogenic action of T0901317 in the vasculature

The anti-inflammatory effect of T0901317 in the vasculature is not restricted to E-selectin. Immunohistochemical staining of intercellular adhesion molecule (ICAM)-1 underlines that T0901317 suppresses endothelial adhesion molecule expression more generally. Whereas in HC 55%±17% of the aortic endothelial cells (EC) expressed ICAM-1, in HC+T0901317 only 22%±7% ($P < 0.05$) of the cells did so (**Fig. 4A, B**). Furthermore, the total number of EC per cross-section with positive p65-NF-κB- or p50-NF-κB-staining (in cytosol and/or nucleus) was strongly reduced in HC+T0901317 (Fig. 4C, D). Also, the number of EC showing nucleus-associated (i.e., active) p65-NF-κB or p50-NF-κB immunoreactivity was strongly and significantly ($P < 0.05$) reduced in HC+T0901317 compared with HC (Fig. 4E, F). These results are further evidence that T0901317 not only lessens the number of NF-κB-positive EC, but also the number of active NF-κB-containing EC, thus providing a rationale for the reduced expression of cellular adhesion molecules and the overall suppressive effect on lesion initiation with T0901317.

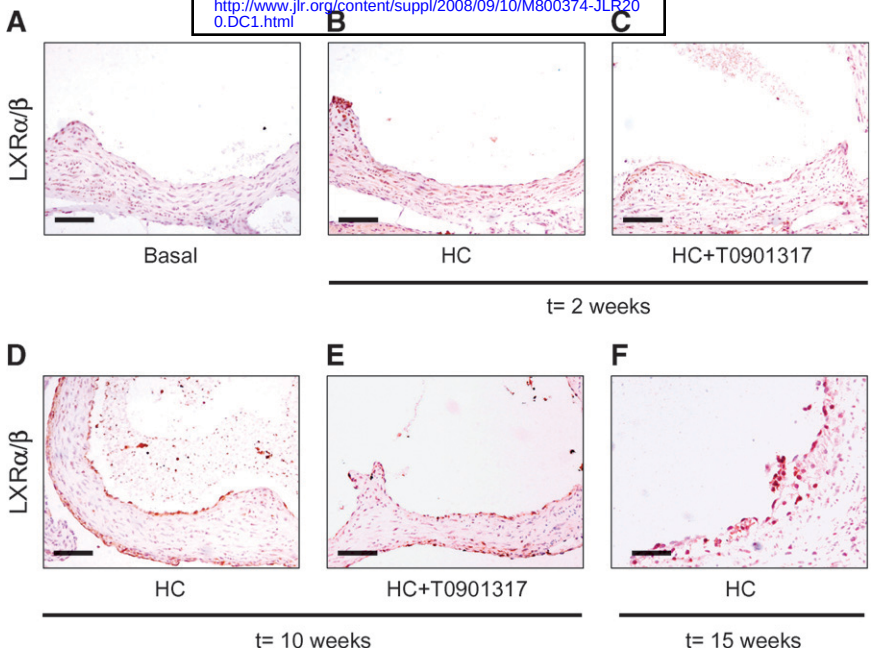

Fig. 3. Vascular LXRα/β expression is induced in cholesterol-fed E3L mice. Representative photomicrographs of immunohistochemical staining of LXRα/β-immunoreactivity (IR) in cross-sections of the aortic root: in basal chow-fed E3L mice (A); after 2 weeks of HC (B) or HC+T0901317 (C); after 10 weeks of HC (D) or HC+T0901317 (E); after 15 weeks of HC (F). Bar = 50 μm.

The T0901317-reduced expression of adhesion molecules is paralleled by diminished recruitment of blood monocytes. As early as 2 weeks after starting HC-treatment, the number of adherent monocytes was significantly increased in HC (7.7 ± 1.7 compared with 4.5 ± 0.7 in chow fed E3L mice (**Fig. 5A**), but not so in HC+T0901317 (4.0 ± 0.9). After 10 weeks, monocyte adhesion was further increased in HC (16.7 ± 4.0; Fig. 5B); monocyte adherence was also elevated in HC+T0901317 (8.3 ± 2.1 vs. 4.0 ± 0.9 at t = 2 weeks; $P < 0.05$), but remained significantly lower than in HC.

Since monocyte-adhesion is a prerequisite, but not sufficient, for formation of early lesions, we subsequently determined lesional macrophage content and macrophage density. Fig. 5C shows that the absolute macrophage-containing lesion area at 10 weeks was substantially (by 85%; $P < 0.05$) reduced in HC+T0901317 compared with HC (1227 ± 507 μm^2 vs. 8238 ± 3168 μm^2). On the other hand, the macrophage density (the macrophage area expressed as percentage of the cross-sectional lesion area) is similar in the two groups (Fig. 5D).

Markedly, in HC+T0901317 lesions are less severe, with lesion progression seemingly blocked at the transition from lesion severity stage II to III (Fig. 2E), a phenotype that is also seen in CD 44-deficient mice (13). CD44 is a cellular adhesion molecule that promotes adhesion and recruitment of monocytes/macrophages and regulates the migration and proliferation of SMC (13, 14). CD44 expression after 10 weeks of HC-treatment is mainly confined to monocytes and macrophage/foam cells in the intima, and expression is further increased and extended to SMC during subsequent atherogenesis progression after 15 weeks (**Fig. 6A, B**). T0901317 strongly and significantly reduced CD44 expression in the vasculature (Figs. 6A–C), both at the mRNA (QRT-PCR analysis) and protein (immunohistochemical analysis) level. In contrast to CD44, T0901317 strongly increased the expression of genes reportedly involved in cholesterol efflux [apoE, ATP binding cassette transporter A1 (ABCA1) and ABCG1; **Table 2**].

Collectively, the data show that in HC+T0901317 lesion number, area, and severity are strongly suppressed with a parallel decrease in monocyte adhesion and SMC migration and proliferation. These effects can at least partly be explained by diminished expression of the adhesion molecules E-selectin, ICAM-1, and CD44, and by an upregulation of factors promoting cholesterol efflux, apoE, ABCA1, and ABCG1.

Effect of T0901317 on pre-existing lesions

Considering the anti-inflammatory and anti-atherosclerotic activities of T0901317, the question arises whether T0901317 can also promote lesion regression. To address this question, E3L mice were fed HC-diet for 18 weeks to induce moderately severe (type III, IV) lesions. One group of animals was then sacrificed (reference group), and two others received a cholesterol-free regression diet (RD) for 8 weeks, supplemented (RD + T0901317) or not (RD) with T0901317. The switch from HC to RD resulted in a fall in total plasma cholesterol from 21.2 ± 5.6 mM to 6.4 ± 2.3 mM ($P < 0.05$, **Fig. 7A**) in the RD group, but no significant change in plasma cholesterol levels was seen in RD + T0901317 (20.7 ± 2.4 mM). Lipoprotein distribution profile analysis (Fig. 7B) shows that the decrease in plasma cholesterol in RD is mainly in the VLDL range, and to a lesser ex-

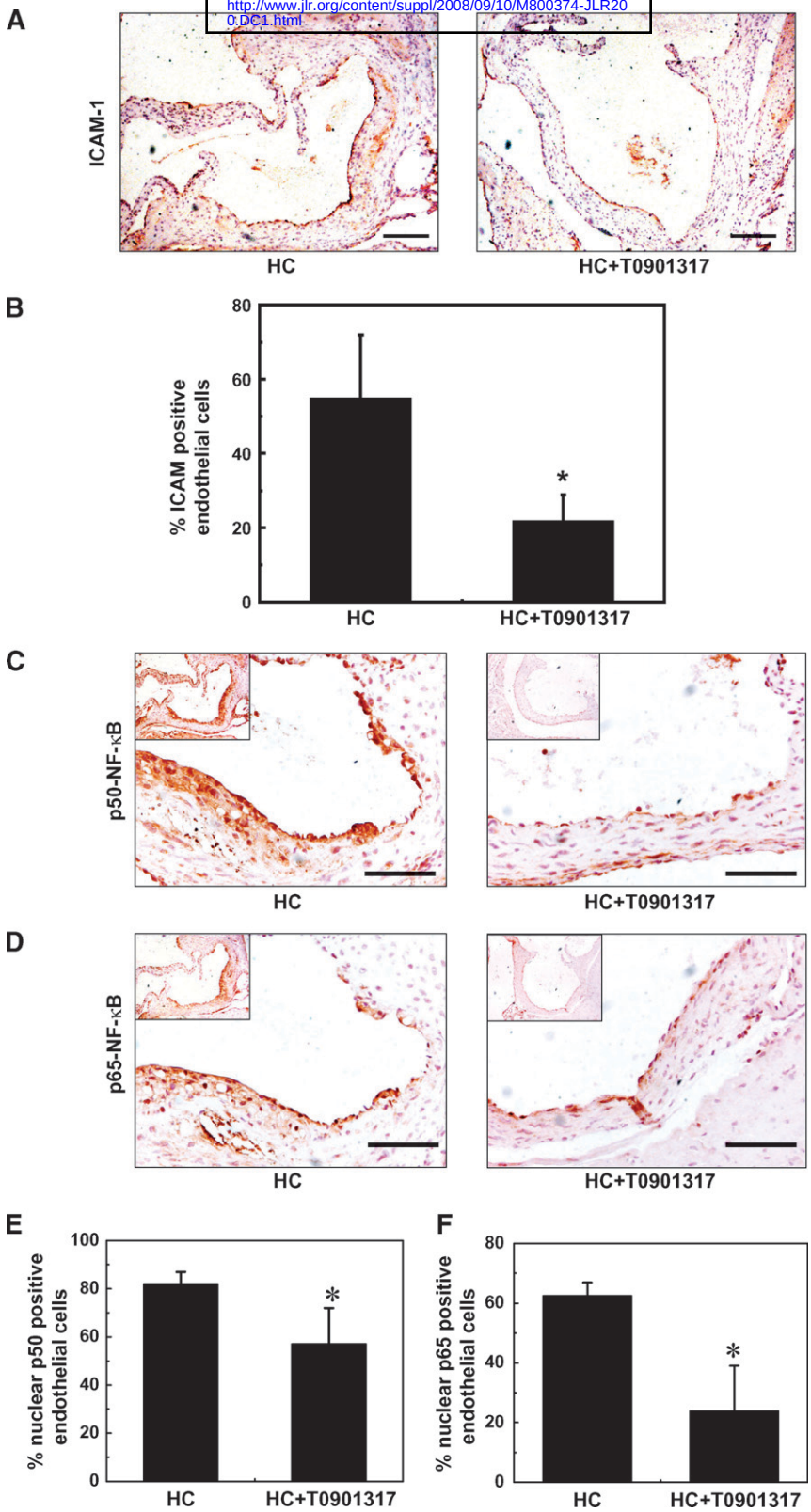

Fig. 4. Effect of T0901317 on vascular intercellular adhesion molecule (ICAM)-1 and NF-κB expression. Representative photomicrographs of immunohistochemical staining of ICAM-1-IR (A), p50-NF-κB-IR (C), and p65-NF-κB-IR (D) after 10 weeks of treatment with HC or HC+T0901317. Percent of ICAM-1-IR positive EC (B), nuclear p50-NF-κB-IR positive EC (E), and nuclear p65-NF-κB-IR positive EC (F) after 10 weeks of treatment with HC or HC+T0901317. * $P < 0.05$ vs. HC. Bar = 100 μm.

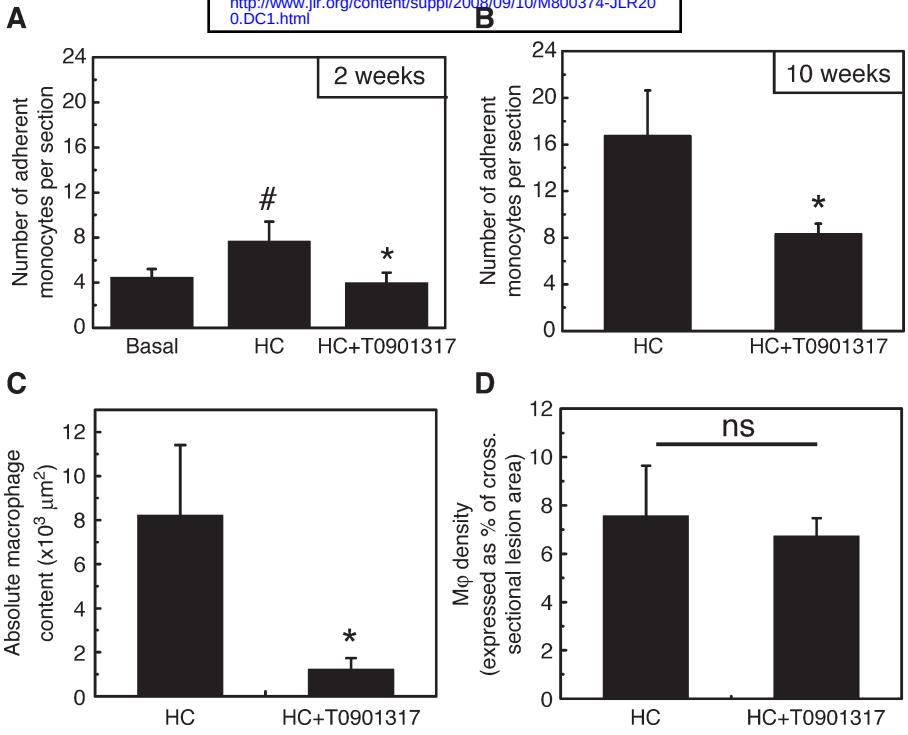

Fig. 5. Effect of T0901317 on aspects of atherogenesis in the aortic valve area. Shown are effects of T0901317 on number of monocytes adhering to endothelium after 2 weeks (A) and 10 weeks of HC (B), on absolute macrophage containing lesion area after 10 weeks (C), and on macrophage density (i.e., macrophage area expressed as percentage of cross-sectional lesion area) after 10 weeks of HC (D). Data are presented as mean ± SD. # $P < 0.05$ vs. chow-fed E3L mice (basal) and * $P < 0.05$ vs. HC.

tent in the IDL/LDL range, but not in the HDL fractions, whereas the profile in RD + T0901317 resembles that seen in HC + T0901317, with an increase of cholesterol in fractions 10–17, corresponding to particles in the IDL/LDL range.

Whereas lesion area in RD (85,924 ± 31,016 μm^2) was not significantly decreased as compared with the reference group (97,203 ± 16,432 μm^2), it was markedly reduced (by 76%) in RD+T0901317 (20,699 ± 7,995 μm^2; $P < 0.05$; Fig. 7C).

In RD and RD+T0901317, a strong decrease in the plaque content of foam cells was observed: from 18,040 ± 3,205 μm^2 in the reference group to 2,876 ± 315 μm^2 in RD ($P < 0.05$) and 363 ± 351 μm^2 in RD+T0901317 ($P < 0.05$; Fig. 7D). Similarly, a significant drop ($P < 0.05$; Fig. 7E) in monocyte adherence was seen in the two groups: from 23 ± 5 monocytes per section (reference) to 16 ± 4 (RD) and 10 ± 2 (RD+T0901317) monocytes per section.

A number of molecular mechanisms underlying regression in mice have been proposed, including macrophage apoptosis (15), CCR7-mediated migration of foam cells to lymph nodes (16, 17), and reverse cholesterol transport (18).

QRT-PCR gene expression analysis (**Table 3**; values normalized for the number of macrophages, with reference mice set at 100%) revealed strongly increased expression of the apoptotic genes caspase-3, BAX, and FAS in aortas from RD mice, and even further enhanced in RD +T0901317 mice. The presence of condensed nuclei in the lesions (Fig. 7F) illustrates the occurrence of ongoing apoptosis in RD + T0901317 mice.

Recently, Trogan et al. (16) reported that the chemokine receptor CCR7 is expressed in foam cells and functionally required for regression. QRT-PCR analysis shows that CCR7 gene expression is significantly increased in RD (225% ± 47%; $P < 0.05$) and even more so in RD + T0901317 (861% ± 132%; $P < 0.01$), indicating that CCR7 could also be a key factor in atherosclerosis regression in the present study. This is underlined by demonstrating enhanced CCR7-stained leukocytes accumulated in the adventitial space (Fig. 7G).

Finally, we sought evidence supportive for increased cholesterol efflux by measuring gene expression of cholesterol efflux pathway-related factors. QRT-PCR analysis of apoE (87% ± 10%), ABCA1 (24% ± 3%; $P < 0.05$), and ABCG1 (62% ± 6%; $P < 0.05$) showed decreased gene expression in RD as compared with the reference group, while T0901317 induced these genes under regression conditions (apoE: 306% ± 20%; ABCA1: 149% ± 24%, and ABCG1: 314% ± 29%; $P < 0.05$, Table 3), even if the macrophage content in RD + T0901317 was stronger decreased than that in RD.

DISCUSSION

We evaluated the effects of an LXR agonist, T0901317 on specific aspects of atherosclerotic lesion progression

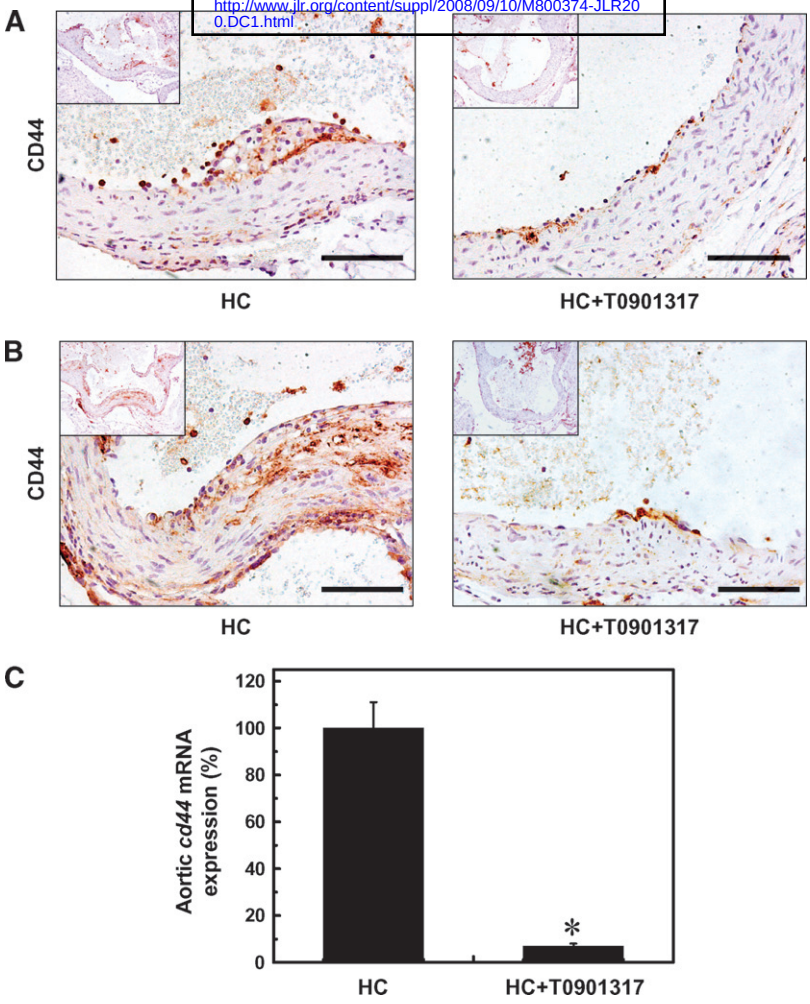

Fig. 6. Effect of T0901317 on vascular CD44 expression. Representative photomicrographs of immunohistochemical staining of CD44-IR in cross-sections of the aortic root after treatment with HC or HC+T0901317 for 10 weeks (A) and 15 weeks (B). Bar = 100 μm. Shown is also aortic *cd44* mRNA expression after 10 weeks of HC or HC+T0901317 (C). * $P < 0.05$ vs. HC.

and regression in E3L mice, a model for atherosclerosis with predictive value for the human situation. In E3L, vascular LXRα and LXRβ expression was induced in aortic EC, SMC, and macrophages under atherogenic dietary conditions. T0901317 strongly suppresses atherosclerotic lesion evolution and promotes lesion regression with respect to lesion number, area, and severity, despite elevated plasma total cholesterol and triglyceride levels. T0901317 exerts its actions at several levels. Under lesion-progressive conditions T0901317 suppresses dietary cholesterol-induced vascular expression of the inflammatory transcription factor, NF-κB, adhesion molecules (E-selectin, ICAM-1, and CD44), monocyte adhesion, and lesional macrophage content. T0901317 also induces the expression of the cholesterol efflux-related genes apoE, ABCA1, and ABCG1, and blocks lesion evolution at the transition from stage II to III.

The ability of T0901317 to promote regression of preexisting atherosclerotic lesions under regressive conditions is linked mechanistically to *i*) increased cholesterol efflux from macrophages in the aortic lesions (through induction of expression of apoE, ABCA1, and ABCG1); *ii*) reduction of macrophage content of the lesions by apoptosis; and iii) increased expression of the chemokine receptor CCR7, a factor functionally required for regression.

The T0901317-induced increase in plasma cholesterol and triglycerides in E3L has also been described previously (19) and is similar to findings in apoE$^{-/-}$ mice (20). The T0901317-induced rise in cholesterol in E3L is confined to particles coeluting with the IDL/LDL fraction and re-

TABLE 2. Effect of T0901317 on vascular gene expression

	HC	HC+ T0901317
apoe	100% ± 11%	211% ± 22.3%[a]
abca1	100% ± 15%	821% ± 211%
abcg1	100% ± 13%	491% ± 109%

HC, high cholesterol. Vascular gene expression of control and T0901317-treated, cholesterol-fed E3L mice. Shown are the average aortic gene expression levels of *apoe, abca1*, and abcg1 at the end of the 10-week treatment period as percentage values relative to corresponding values at the start (t = 0) of the treatment (means ± SD; n = 12 for each group).

[a] $P < 0.05$ vs. HC.

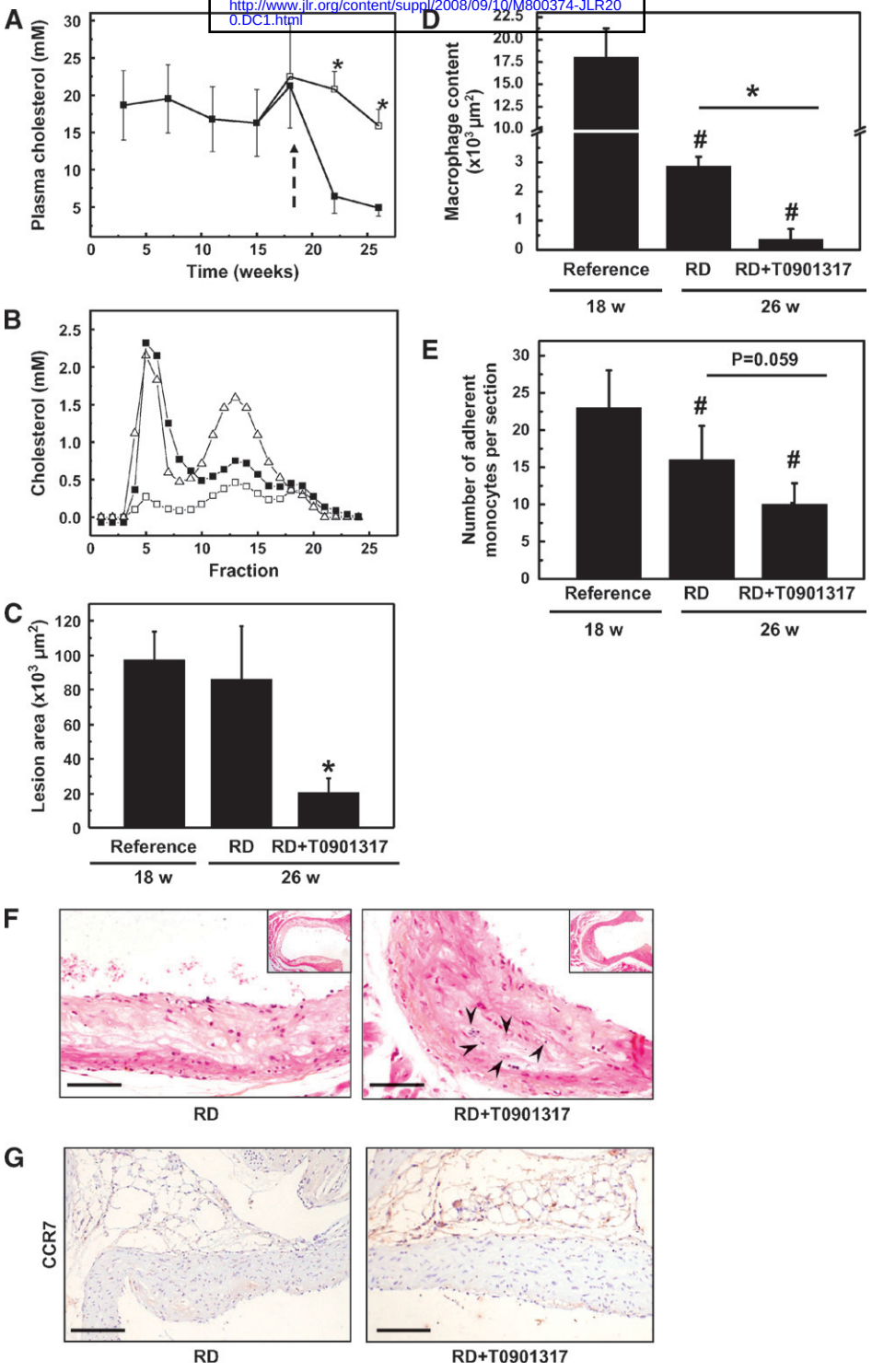

Fig. 7. Effect of T0901317 on aspects of atherosclerotic lesion regression. Shown are plasma cholesterol concentrations during regression period (arrow indicates start of RD feeding), with solid squares indicating RD treatment group and open squares indicating RD+T0901317 group (A). Data are represented as mean ± SD, * $P < 0.05$ vs. RD. Lipoprotein distribution profiles of the two experimental groups (n = 8 for each group) after 8 weeks of RD (open squares) or RD+T0901317 (solid squares) (B). For comparison, the lipoprotein profile of pooled plasma of the reference group (n = 10; t = 18 weeks) is also shown (triangles); total cross-sectional lesion area of reference, RD, and RD+T0901317 groups, with data representing mean values ± SEM (n = 8 per group) (C); absolute macrophage containing lesion area, with data representing mean values ± SEM (n = 8 mice per group) (D); number of monocytes adhering to endothelium, with data representing mean values ± SEM (n = 8 mice per group) (E); representative photomicrographs illustrating condensed nuclei (arrowheads) (F); representative photomicrographs of immunohistochemical staining of adventitial CCR7-IR (G).

TABLE 3. Effect of T0901317 on vascular gene expression under regressive conditions

	t = 18 weeks	Regression t = 26 weeks	
	Reference	RD	RD+T0901317
fas	100% ± 4%	291% ± 11%[a]	2726% ± 148%[a,b]
bax	100% ± 6%	876% ± 87%[a]	3072% ± 374%[a,b]
casapse3	100% ± 5%	434% ± 34%[a]	2173% ± 386%[a,b]
ccr7	100% ± 16%	225% ± 47%[a]	861% ± 132%[a,b]
Apoe	100% ± 11%	87% ± 10%	306% ± 20%[a,b]
abca1	100% ± 8%	24% ± 3%[a]	149% ± 24%[a,b]
Abcg1	100% ± 17%	62% ± 6%[a]	314% ± 29%[a,b]

Vascular gene expression of control and T0901317-treated E3L mice on a cholesterol-free, regressive diet (RD). Shown are average aortic gene expression levels of cholesterol-efflux-related (*apoe, abca1,* and abcg1) and apoptosis/regression-related genes (*fas, bax, caspase-3,* and *ccr7*) at the end of the regression period (t = 26 weeks) relative to reference group, which was set at 100%. Values are normalized for aortic monocyte/macrophage content (means ± SD).

[a] $P < 0.05$ vs. reference.

[b] $P < 0.05$ vs. RD.

sembles findings described for fenofibrate-treated E3L mice (21). The induced fraction contains mainly the apolipoprotein apoE, to a minor extent apoB, and not apoA1. In contrast, the T0901317-induced increase in cholesterol in apoE$^{-/-}$ was in HDL and accompanied by a marked increase in apoA1, but not ApoB levels (20). Interestingly, the apolipoprotein composition and size of the T0901317-induced particle in E3L is comparable to that induced by T0901317 in C57/Bl6 mice which was designated "enlarged HDL" (22). The particle also shows the characteristics of HDL1, which has been suggested to be involved in apoA1-independent cholesterol efflux, possibly sustained by apoE (23, 24).

Different effects of LXR agonists on cholesterol have been described in LDLr$^{-/-}$ mice. In one report, T0901317 did not affect plasma total cholesterol levels in LDLr$^{-/-}$ mice fed an atherogenic diet (8), and in other studies a decrease in plasma cholesterol levels was observed with LXR agonists (5, 6).

A common finding in studies using T0901317 or other LXR ligands is the rise in triglyceride levels, which can be ascribed to the induction of the transcription factor SREBP-1 and its target genes FAS and SCD, two key enzymes involved in lipogenesis (3, 4). Noteworthy, T0901317 also is a high-affinity ligand for the xenobiotic receptor, pregnane-X-receptor (PXR). Because PXR and the LXRs are coexpressed in liver and PXR plays an important role in lipid metabolism, some of the hepatic effects of T0901317 may have resulted from simultaneous stimulation of LXR and PXR activation (25). Importantly, vascular effects of T0901317 reported here most likely reflect LXR activation only since CD36, a PXR target (26), was not induced by T0901317 in E3L mice (data not shown).

Our finding that T0901317 strongly suppresses atherosclerotic lesion evolution in E3L mice is in line with previous gain-of-function and loss-of-function studies (7) and results obtained in apoE$^{-/-}$ and LDLr$^{-/-}$ mice with T0901317 and the LXR agonist GW3965 (5, 8). The present study reveals several levels of anti-atherosclerotic action of T0901317. First, a strong reduction of aortic inflammation is reflected by diminished vascular endothelial NF-κB activity, adhesion molecule expression (E-selectin, ICAM-1, and CD44), monocyte adhesion, and lesional macrophage content, all in the absence of systemic inflammation (cf. SAA). Second, T0901317 strongly increases gene expression of factors important for cholesterol efflux from vascular macrophages (apoE, ABCA1, and ABCG1). ABCA1 mediates cholesterol efflux from macrophages to lipid-free apoA1 (27), whereas ABCG1 is a mediator of macrophage cholesterol efflux to mature HDL in vitro (28). Up-regulation of ABCA1 and ABCG1 in the vasculature has previously been suggested to contribute to the anti-atherogenic capacity of T0901317(5;8). Another LXR agonist, GW3965, was shown to increase aortic expression of ABCA1 and ABCG1 in apoE$^{-/-}$ mice (5).

Third, T0901317 blocked lesion progression from lesion severity stage II to III, characterized by the absence of SMC in the cap (12). Proliferation and migration of SMC from the media toward the intima, a hallmark of type III lesions, is a key event in lesion progression and regulated by CD44 (29, 30). The detected down-regulation of CD44 by T0901317 in our study may thus provide an explanation for the observed blockage of lesion progression.

Atherosclerosis regression is an important clinical goal, but mouse studies on regression are few. We observed that under dietary cholesterol-free ("regressive") conditions, there was a rapid loss of plaque foam cells from existing plaques, and this process was further enhanced by T0901317. In line with a previous study in E3L mice, macrophage disappearance preceded reduction in plaque size under regressive conditions (11). Remarkably, the effect of T0901317 on plaque regression occurred while plasma cholesterol level and lipoprotein profile were similar to those found with T0901317 under progressive (HC) conditions. Also, monocyte adherence in the presence of T0901317 was not different between regressive and progressive conditions.

Three processes were identified that could be relevant for explaining the T0901317-stimulated disappearance of macrophages. First, the disappearance of macrophages could be the result of apoptosis. Indeed, we found evidence for increased number of apoptotic bodies with a parallel up-regulation of pro-apoptotic genes (caspase-3, BAX, and FAS) in the aorta. Second, T0901317 enhances gene expression of reverse cholesterol transport markers, apoE, ABCA1, and ABCG1. This is of relevance because it is thought that the elevated plasma membrane cholesterol content in foam cells inhibits cell migration (31). Since plaque progression may result in part from long-term retention of foam cells in the plaque, promoting emigration of foam cells from atherosclerotic lesions through lowering cellular cholesterol content might lead to plaque regression. Third, findings from a study by Trogan et al. (16) raised the possibility that, during regression, foam cells acquire dendritic cell characteristics that permit them to migrate to draining lymph nodes. This migration depends on the chemokine receptor CCR7, which might become up-regulated in foam cells in plaques undergoing regression. When CCR7 function was abrogated in vivo by

treatment with antibodies to CCR7 ligands CCL19 and CCL21, lesion size and foam cell content were substantially preserved. In line with this, we found that CCR7 expression in the vasculature is located at the adventitial space and is increased 2-fold when regression is induced by RD and 8-fold by RD+T0901317, despite the decreases in macrophage content. Concomitantly, increases in hepatic CCL19 and CCL21 expression were observed (data not shown).

In summary, our findings show a comprehensive analysis of the beneficial effects of T0901317 on lesion evolution and regression in E3L mice and provide plausible mechanisms for its mode of action, including stimulation of cholesterol efflux-related genes and suppression of the inflammatory state. The data also revealed CCR7 induction in foam cells, a chemokine receptor reportedly functionally required for regression. LXR agonists could thus contribute in abrogating (pre-existing) atherosclerosis.

REFERENCES

1. Braunwald, E. 1997. Shattuck lecture–cardiovascular medicine at the turn of the millennium: triumphs, concerns, and opportunities. *N. Engl. J. Med.* **337:** 1360–1369.
2. Libby, P., P. M. Ridker, and A. Maseri. 2002. Inflammation and atherosclerosis. *Circulation.* **105:** 1135–1143.
3. Schultz, J. R., H. Tu, A. Luk, J. J. Repa, J. C. Medina, L. Li, S. Schwendner, S. Wang, Thoolen, D. J. Mangelsdorf, et al. 2000. Role of LXRs in control of lipogenesis. *Genes Dev.* **4:** 2831–2838.
4. Zelcer, N. and P. Tontonoz. 2006. Liver X receptors as integrators of metabolic and inflammatory signaling. *J. Clin. Invest.* **116:** 607–614.
5. Joseph, S. B., E. McKilligin, L. Pei, M. A. Watson, A. R. Collins, B. A. Laffitte, M. Chen, G. Noh, J. Goodman, G. N. Hagger, et al. 2002. Synthetic LXR ligand inhibits the development of atherosclerosis in mice. *Proc. Natl. Acad. Sci. USA.* **99:** 7604–7609.
6. Levin, N., E. D. Bischoff, C. L. Daige, D. Thomas, C. T. Vu, R. A. Heyman, R. K. Tangirala, and I. G. Schulman. 2005. Macrophage liver X receptor is required for antiatherogenic activity of LXR agonists. *Arterioscler. Thromb. Vasc. Biol.* **25:** 135–142.
7. Tangirala, R. K., E. D. Bischoff, S. B. Joseph, B. L. Wagner, R. Walczak, B. A. Laffitte, C. L. Daige, D. Thomas, R. A. Heyman, D. J. Mangelsdorf, et al. 2002. Identification of macrophage liver X receptors as inhibitors of atherosclerosis. *Proc. Natl. Acad. Sci. USA.* **99:** 11896–11901.
8. Terasaka, N., A. Hiroshima, T. Koieyama, N. Ubukata, Y. Morikawa, D. Nakai, and T. Inaba. 2003. T-0901317, a synthetic liver X receptor ligand, inhibits development of atherosclerosis in LDL receptor-deficient mice. *FEBS Lett.* **536:** 6–11.
9. Zadelaar, S., R. Kleemann, L. Verschuren, J. de Vries-van der Weij, J. van der, Hoorn, H. M. Princen, and T. Kooistra. 2007. Mouse models for atherosclerosis and pharmaceutical modifiers. *Arterioscler. Thromb. Vasc. Biol.* **27:** 1706–1721.
10. Kleemann, R., L. Verschuren, M. J. van Erk, Y. Nikolsky, N. H. Cnubben, E. R. Verheij, A. K. Smilde, H. F. Hendriks, S. Zadelaar, G. J. Smith, et al. 2007. Atherosclerosis and liver inflammation induced by increased dietary cholesterol intake: a combined transcriptomics and metabolomics analysis. *Genome Biol.* **8:** R200.
11. Gijbels, M. J., M. van der Cammen, L. J. van der Laan, J. J. Emeis, L. M. Havekes, M. H. Hofker, and G. Kraal. 1999. Progression and regression of atherosclerosis in APOE3-leiden transgenic mice: an immunohistochemical study. *Atherosclerosis.* **143:** 15–25.
12. Stary, H. C. 2000. Natural history and histological classification of atherosclerotic lesions: an update. *Arterioscler. Thromb. Vasc. Biol.* **20:** 1177–1178.
13. Zhao, L., J. A. Hall, N. Levenkova, E. Lee, M. K. Middleton, A. M. Zukas, D. J. Rader, J. J. Rux, and E. Pure. 2007. CD44 regulates vascular gene expression in a proatherogenic environment. *Arterioscler. Thromb. Vasc. Biol.* **27:** 886–892.
14. Cuff, C. A., D. Kothapalli, I. Azonobi, S. Chun, Y. Zhang, R. Belkin, C. Yeh, A. Secreto, R. K. Assoian, D. J. Rader, et al. 2001. The adhesion receptor CD44 promotes atherosclerosis by mediating inflammatory cell recruitment and vascular cell activation. *J. Clin. Invest.* **108:** 1031–1040.
15. Wang, B. Y., H. K. Ho, P. S. Lin, S. P. Schwarzacher, M. J. Pollman, G. H. Gibbons, P. S. Tsao, and J. P. Cooke. 1999. Regression of atherosclerosis: role of nitric oxide and apoptosis. *Circulation.* **99:** 1236–1241.
16. Trogan, E., J. E. Feig, S. Dogan, G. H. Rothblat, V. Angeli, F. Tacke, G. J. Randolph, and E. A. Fisher. 2006. Gene expression changes in foam cells and the role of chemokine receptor CCR7 during atherosclerosis regression in apoe-deficient mice. *Proc. Natl. Acad. Sci. USA.* **103:** 3781–3786.
17. Llodra, J., V. Angeli, J. Liu, E. Trogan, E. A. Fisher, and G. J. Randolph. 2004. Emigration of monocyte-derived cells from atherosclerotic lesions characterizes regressive, but not progressive, plaques. *Proc. Natl. Acad. Sci. USA.* **101:** 11779–11784.
18. Cuchel, M., and D. J. Rader. 2006. Macrophage reverse cholesterol transport: key to the regression of atherosclerosis? *Circulation.* **113:** 2548–2555.
19. Grefhorst, A., B. M. Elzinga, P. J. Voshol, T. Plosch, T. Kok, V. W. Bloks, F. H. van der Sluijs, L. M. Havekes, J. A. Romijn, H. J. Verkade, et al. 2002. Stimulation of lipogenesis by pharmacological activation of the liver X receptor leads to production of large, triglyceride-rich very low density lipoprotein particles. *J. Biol. Chem.* **277:** 34182–34190.
20. Dai, X., X. Ou, X. Hao, D. Cao, Y. Tang, Y. Hu, X. Li, and C. Tang. 2007. Effect of T0901317 on hepatic proinflammatory gene expression in apoE−/− mice fed a high-fat/high-cholesterol diet. *Inflammation.* **30:** 105–117.
21. Kooistra, T., L. Verschuren, J. de Vries-van der Weij, W. Koenig, K. Toet, H. M. Princen, and R. Kleemann. 2006. Fenofibrate reduces atherogenesis in apoE*3Leiden mice: evidence for multiple antiatherogenic effects besides lowering plasma cholesterol. *Arterioscler. Thromb. Vasc. Biol.* **26:** 2322–2330.
22. Jiang, X. C., T. P. Beyer, Z. Li, J. Liu, W. Quan, R. J. Schmidt, Y. Zhang, W. R. Bensch, P. I. Eacho, and G. Cao. 2003. Enlargement of high density lipoprotein in mice via liver X receptor activation requires apolipoprotein E and is abolished by cholesteryl ester transfer protein expression. *J. Biol. Chem.* **278:** 49072–49078.
23. Gruen, M. L., M. R. Plummer, W. Zhang, K. A. Posey, M. F. Linton, S. Fazio, and A. H. Hasty. 2005. Persistence of high density lipoprotein particles in obese mice lacking apolipoprotein A-I. *J. Lipid Res.* **46:** 2007–2014.
24. Vaisman, B. L., G. Lambert, M. Amar, C. Joyce, T. Ito, R. D. Shamburek, W. J. Cain, J. Fruchart-Najib, E. D. Neufeld, A. T. Remaley, et al. 2001. ABCA1 overexpression leads to hyperalphalipoproteinemia and increased biliary cholesterol excretion in transgenic mice. *J. Clin. Invest.* **108:** 303–309.
25. Mitro, N., L. Vargas, R. Romeo, A. Koder, and E. Saez. 2007. T0901317 is a potent PXR ligand: implications for the biology ascribed to LXR. *FEBS Lett.* **581:** 1721–1726.
26. Zhou, J., Y. Zhai, Y. Mu, H. Gong, H. Uppal, D. Toma, S. Ren, R. M. Evans, and W. Xie. 2006. A novel pregnane X receptor-mediated and sterol regulatory element-binding protein-independent lipogenic pathway. *J. Biol. Chem.* **281:** 15013–15020.
27. Wang, N., D. L. Silver, P. Costet, and A. R. Tall. 2000. Specific binding of apoA-I, enhanced cholesterol efflux, and altered plasma membrane morphology in cells expressing ABC1. *J. Biol. Chem.* **275:** 33053–33058.
28. Wang, N., D. Lan, W. Chen, F. Matsuura, and A. R. Tall. 2004. ATP-binding cassette transporters G1 and G4 mediate cellular cholesterol efflux to high-density lipoproteins. *Proc. Natl. Acad. Sci. USA.* **101:** 9774–9779.
29. Lazaar, A. L., S. M. Albelda, J. M. Pilewski, B. Brennan, E. Pure, and R. A. Panettieri, Jr. 1994. T lymphocytes adhere to airway smooth muscle cells via integrins and CD44 and induce smooth muscle cell DNA synthesis. *J. Exp. Med.* **180:** 807–816.
30. Jain, M., Q. He, W. S. Lee, S. Kashiki, L. C. Foster, J. C. Tsai, M. E. Lee, and E. Haber. 1996. Role of CD44 in the reaction of vascular smooth muscle cells to arterial wall injury. *J. Clin. Invest.* **98:** 877.
31. Nagao, T., C. Qin, I. Grosheva, F. R. Maxfield, and L. M. Pierini. 2007. Elevated cholesterol levels in the plasma membranes of macrophages inhibit migration by disrupting RhoA regulation. *Arterioscler. Thromb. Vasc. Biol.* **27:** 1596–1602.